DYNAMIC SIMULATION OF STARTING AND CHOPPER SPEED CONTROL OF WOUND-ROTOR INDUCTION MOTOR

SALEH AL-JUFOUT, KAMAL KHANDAKJI

Department of Electrical Engineering, Faculty of Engineering, Tafila Technical University, Tafila, Jordan
E-mails: drjufout@yahoo.com, drkhandakji@yahoo.com

Abstract: This research article presents dynamic simulation of starting and speed-control of the wound-rotor induction motor based on mathematical modelling. The behaviour of this motor has been represented by a system of differential equations for flux linkages and angular velocity. The differential equations for the flux linkages have been expressed in the Cartesian system of coordinates, which decreased the number of equations by one third. Starting and different speed-control modes of the motor have been computed and analyzed. The developed model has been verified by direct comparison with experimental results obtained in the laboratory.

Keywords: Wound-Rotor Motor, Starting, Speed Control, Dynamic Simulation, Cartesian Coordinates

1. INTRODUCTION

The availability of special-purpose simulation languages, massive computing capabilities at a decreasing cost per operation and advances in simulation methodologies have made simulation one of the most widely used and accepted tools in operation research and system analysis. Simulation enables the study of the internal interaction of a complex system, or of a subsystem within a complex system. The knowledge gained in designing a simulation model may be of great value toward suggesting improvement in the system under investigation and by changing simulation inputs and observing the resulting output; valuable insight may be obtained in which variables are most important and how variables interact.

Since 1999, in the laboratory of electrical machines at Tafila Technical University, a significant amount of research was devoted to the three-phase induction motor: direct starting (Al-Jufout, 1999; Al-Jufout, 2000); open-circuit transition wye-delta starting (Al-Jufout, 2003); autotransformer reduced voltage starting (Al-Jufout, 2002); variable-frequency drive (Al-Jufout, 2000); reclosing (Al-Jufout, 2000); symmetrical and asymmetrical modes of operation (Al-Jufout, 2003), but we felt that the work was incomplete until the operation of the wound-rotor induction motor was simulated. This simulation is the subject of the proposed research article.

Although a wound-rotor motor costs more than a squirrel-cage one, it offers many advantages: the wye-connected rheostat with a common lever provides speed control, torque adjustment at locked rotor and current limiting during starting and acceleration (Wildi, 2006). Recently, many articles about the wound-rotor induction motor are published. In (Sen, 1990) a comprehensive review of the state of the art in the field of electric motor drives and control strategies is presented. It is pointed out that drive technology has seen impressive growth during the last three decades. In (Arkan, 2005) two orthogonal axis models for simulation of three-phase induction motors having asymmetrical windings and inter-turn short circuits on the stator are presented. The first model assumes that each stator phase winding has a different number of turns. The second model assumes that each phase has two windings in series, representing the unaffected portion and the shorted portion, respectively. In (Zhang et al, 2004) the method to implement the dynamic simulation for an induction motor vector-control system is explained.

A unified method for modelling and simulation of electrical drives using state-space formulation in MATLAB/Simulink is presented in (Hoang, 2001), where the proposed method has been successfully implemented in a simulation package called "Power System Blockset" for use in MATLAB/Simulink environment and an application example of a direct torque control of the induction motor drive is presented. In (Cunha et al, 2005) the model of the induction machine including rotor bar and end-ring faults, with a minimum of computational complexity is developed. And a technique is being developed which will allow the detection and identification of specific faults within 3-phase induction motors during the starting transient as explained in (Elder et al, 1989). In (Khandakji and Zdrozis, 2005), a mathematical analysis of hoisting electric drive system incorporating three-phase reversible voltage-

controlled wound-rotor induction motor is illustrated. In (Shi et al, 1999; Seker and Ayaz, 2003; Lagonotte et al, 1999; Boglietti and Carpaneto, 2001; O'Sullivan, 2004; Ayasun and Nwankpa, 2005), different models of the induction motor are developed, but each of the above-mentioned articles solves one certain problem and mostly for steady-state conditions. Although the speed control by the rheostat controller is relatively an old technology, it is still found in industry, thus, the objective of this paper is to develop a comprehensive mathematical model for simulating both the transient and steady-state operating conditions of the wound-rotor induction motor, such as: unloaded and loaded starting with current-, speed- or time-controlled starting rheostat, short-circuit at the terminals of the motor, sudden load change (fixed or variable load), speed control and any other symmetrical operating conditions.

2. DYNAMIC MODEL OF THE WOUND-ROTOR MOTOR

The three-phase, wound-rotor induction motor can be mathematically modeled by representing it as a system of differential equations for flux linkages and angular velocity. The state equations can be expressed in Cartesian coordinate system (α, β) as follows:

$$\frac{d\lambda_{S\alpha}}{dt} = v_{S\alpha} - \frac{R_S}{L_{\sigma S}}(\lambda_{S\alpha} - \lambda_{\mu\alpha}) \quad (1)$$

$$\frac{d\lambda_{S\beta}}{dt} = v_{S\beta} - \frac{R_S}{L_{\sigma S}}(\lambda_{S\beta} - \lambda_{\mu\beta}) \quad (2)$$

$$\frac{d\lambda_{R\alpha}}{dt} = -\frac{R_R + R_{Ext}}{L_{\sigma R}}(\lambda_{R\alpha} - \lambda_{\mu\alpha}) - \omega\ \lambda_{R\beta} \quad (3)$$

$$\frac{d\lambda_{R\beta}}{dt} = -\frac{R_R + R_{Ext}}{L_{\sigma R}}(\lambda_{R\beta} - \lambda_{\mu\beta}) + \omega\ \lambda_{R\alpha} \quad (4)$$

$$\frac{d\omega}{dt} = \frac{1}{J}(\tau_e - \tau_m) \quad (5)$$

where

$\lambda_{S\alpha}, \lambda_{R\alpha}, \lambda_{S\beta}, \lambda_{R\beta}$ - The flux linkages of the stator and the rotor circuits in α and β coordinates respectively;

R_S, R_R, R_{Ext} - The resistances of the stator, rotor circuits and the external starting rheostat respectively;

$L_{\sigma S}, L_{\sigma R}$ - The leakage inductances of the stator and the rotor circuits respectively;

$v_{S\alpha}, v_{S\beta}$ - The applied voltages in α and β coordinates respectively;

$\lambda_{\mu\alpha}, \lambda_{\mu\beta}$ - The flux linkages of the magnetization branch in α and β coordinates respectively;

ω - The angular velocity of the motor;

J - The combined rotor and mechanical load inertia;

τ_e, τ_m - The electromagnetic and the mechanical torque respectively.

The electromagnetic torque and the flux linkages of the magnetization branch can be calculated as follows:

$$\tau_e = \frac{1}{L_{\sigma S}}\left[\lambda_{S\beta} k_R \lambda_{R\alpha} - \lambda_{S\alpha} k_R \lambda_{R\beta}\right] \quad (6)$$

$$\lambda_{\mu\alpha} = k_S \lambda_{S\alpha} + k_R \lambda_{R\alpha} \quad (7)$$

$$\lambda_{\mu\beta} = k_S \lambda_{S\beta} + k_R \lambda_{R\beta} \quad (8)$$

Where the contributing coefficients can be calculated as follows:

$$k_S = \frac{1}{L_{\sigma S}}\left[\frac{1}{L_{\sigma S}} + \frac{1}{L_\mu} + \frac{1}{L_{\sigma R}}\right]^{-1} \quad (9)$$

$$k_R = \frac{1}{L_{\sigma R}}\left[\frac{1}{L_{\sigma S}} + \frac{1}{L_\mu} + \frac{1}{L_{\sigma R}}\right]^{-1} \quad (10)$$

where

L_μ - The inductance of the magnetization branch.

The stator currents can be calculated as follows:

$$i_{S\alpha} = \frac{\lambda_{S\alpha} - \lambda_{\mu\alpha}}{L_{\sigma S}} \quad (11)$$

$$i_{S\beta} = \frac{\lambda_{S\beta} - \lambda_{\mu\beta}}{L_{\sigma S}} \quad (12)$$

The active and reactive powers can be determined by the following formulas, by which the power factor with which the motor operates can also be calculated:

$$P = v_{S\alpha} i_{S\alpha} + v_{S\beta} i_{S\beta} \quad (13)$$

$$Q = v_{S\beta} i_{S\alpha} - v_{S\alpha} i_{S\beta} \quad (14)$$

The rheostat starter and speed controller with the use of contactors or a common lever can be simply modeled by logic condition operators or commands. Nowadays, the circuit shown in figure 1 is more widely used.

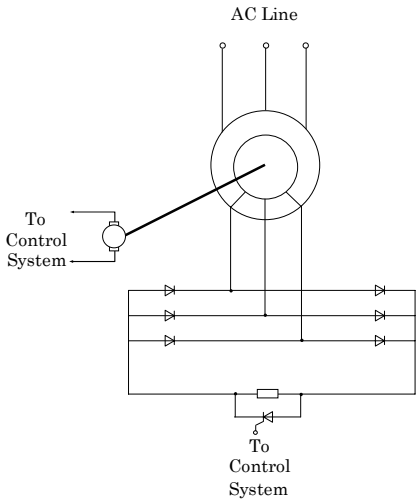

Figure 1: Chopper speed control of the wound-rotor induction motor

In addition to speed control, torque adjustment at locked rotor and current limiting during starting and acceleration, this circuit provides better speed regulation, smoothness and the ability to be used in closed-loop control system for torque and speed control, where the equivalent resistance of the external resistance is inversely proportional to the duty cycle of the chopper. The duty cycle can be calculated as follows:

$$D = \frac{T_{on}}{T_{cycle}} = \frac{T_{on}}{T_{on} + T_{off}} \quad (15)$$

where

T_{on}, T_{off} - The duration during which the thyristor is on and off respectively.

The maximum value of the external rheostat, in per unit, can be calculated as follows:

$$R_{Ext.\max} = \sqrt{R_S^2 + X_{\sigma S}^2} - R_R \quad (16)$$

where the reactance of the stator equals its leakage inductance in per unit.

Figure 2 shows the closed-loop control system for torque- and speed control of the wound-rotor motor, where the PID speed and rotor-current controllers allow speed and torque control in transient and steady-state conditions. The rotor-current controller maintains constant dynamic (accelerating or decelerating) torque in transients, thus minimizing the duration of the transients. Here the speed controller maintains constant motor speed with variations of the load.

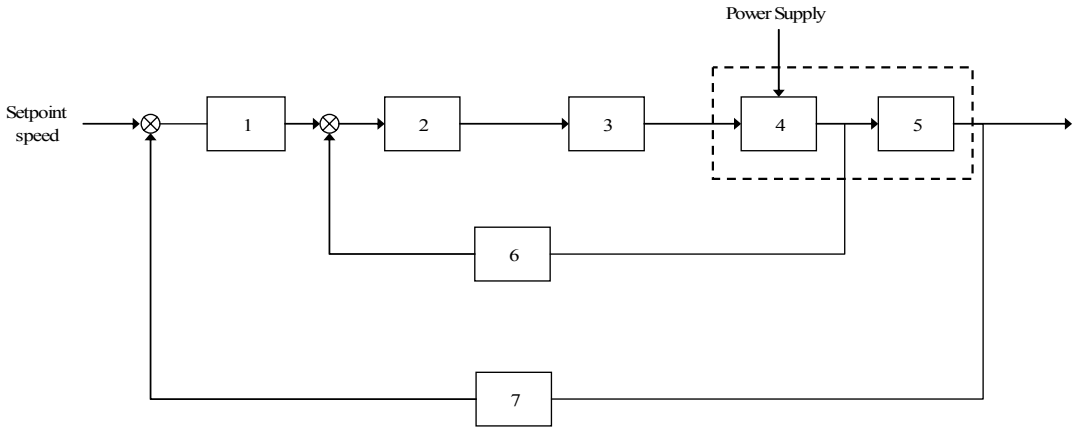

Figure 2: Closed-loop control system for torque and speed control of the wound-rotor motor: 1) speed-controller, 2) rotor-current controller, 3) chopper, 4) wound-rotor, 5) mechanical part of the motor, 6) current sensor, 7) speed sensor

Comparing the above described model with the existing ones, the following advantages can be obtained:

- It is comprehensive for simulation of many symmetrical operating conditions.
- It consists only of five differential equations.
- The coefficients in the differential

equations do not depend on the angular velocity; consequently there is no need to recalculate them at every step of solution.
- It can be used for both transient and steady-state analysis.
- Its parameters can simply be identified in per unit by using the engineering methods.

Regardless of these advantages the mentioned above numerical model can be used only for symmetrical modes analysis, due to the use of Cartesian coordinate system.

3. EXPERIMENTAL SETUP

The tested motor is a standard three-phase wound-rotor induction motor for which the ratings are listed in table 1. The motor is connected to a general power supply for laboratory conditions. The load is quadratic and has a torque characteristic nearly proportional to the square of the motor speed. Voltage, current and speed were measured and recorded using a digital oscilloscope. Two tests were performed:
- Direct starting with starting rheostat short-circuited.
- Loaded starting with speed-controlled starting rheostat.

Table 1: Rated values of the tested wound-rotor induction motor

Parameter	Value
Rated Voltage, V	24
Rated Current, A	10
Rated Power, W	200
Rated Speed, rpm	2800
Power Factor	0.75
Frequency, Hz	50

The parameters of the equivalent circuit were determined experimentally and are listed in table 2.

Table 2: Parameters of the equivalent circuit of the tested motor

Parameter	Value, Ω
Resistance of the stator	0.029
Leakage reactance of the stator	0.139
Resistance of the rotor	0.028
Leakage reactance of the rotor	0.025
Reactance of the magnetization branch	5.115

Comparing the results measured in the laboratory for the above mentioned experiments with the modelling results validates the developed model, where the error is within the range of (2-5)%.

4. RESULTS AND DISCUSSION

The above mentioned differential equations can be solved by fourth-order Runge-Kutta method (Richard and Douglas, 2002). The applied voltages are given and the equivalent circuit parameters (resistances and inductances) can be defined in per unit by engineering methods (Fitzgerald et al, 1992).

Simulation in this paper is performed in per unit values. Table 3 displays the formulas used to determine the base values used in the above-described model.

Table 3: Per unit system and values used for the tested motor

Base Parameter	Formula	Value for the Tested Motor
Voltage, V	$V_{base} = \sqrt{\frac{2}{3}} \cdot V_{rated}$	19.59
Current, A	$I_{base} = \sqrt{2} \cdot I_{rated}$	14.14
Power, VA	$S_{base} = \frac{3}{2} \cdot V_{base} I_{base}$	514.5
Impedance, Ω	$Z_{base} = \frac{V_{base}}{I_{base}}$	1.39
Angular Velocity, rad/sec.	$\omega_{base} = \omega_{syn.}$	314
Speed, rpm	$n_{base} = n_{syn.}$	3000
Inductance, H	$L_{base} = \frac{Z_{base}}{\omega_{base}}$	0.004
Torque, N.m	$\tau_{base} = \frac{S_{base} \cdot P}{\omega_{base}}$	1.323
Moment of Inertia, N.m.sec.^{2}	$J_{base} = \frac{S_{base} \cdot P^2}{\omega^3_{base}}$	0.0000134
Time, sec.	$t_{base} = \frac{1}{\omega_{base}}$	1/314

Table 4 shows the parameters of the equivalent circuit of the tested motor calculated in per unit.

Table 4: Parameters of the equivalent circuit of the tested motor

Parameter	Value, p.u.
Resistance of the stator	0.021
Leakage inductance of the stator	0.1
Resistance of the rotor	0.02
Leakage inductance of the rotor	0.0178
Magnetization branch inductance	3.68

The mechanical load can be either a constant or as a function of the angular velocity (fan or pump load). In this research the loading coefficient is given by the following formula:

$$k = 0.1 + 0.7\omega^2 \qquad (17)$$

To demonstrate the effect of the starting rheostat, the motor, firstly, is started with short-circuited starting rheostat. Figure 3 shows the phase time-domain starting current, where the inrush current is 8.56 p.u. and the amplitude of the starting current is about 7.5 p.u. The starting duration is 1.98 sec.

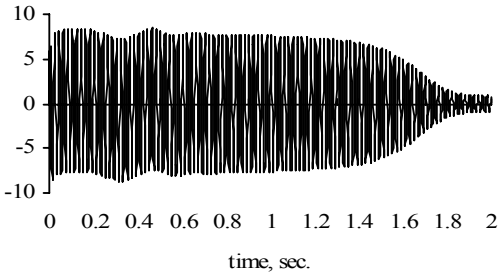

Figure 3: The stator phase current of the wound-rotor motor at start-up with short-circuited starting rheostat

Figure 4 shows the electromagnetic torque of the motor at start-up with short-circuited starting rheostat, where the inrush torque is 4.94 p.u. and the starting torque is about 1.9 p.u. Figure 3 and figure 4 also show the steady-state conditions, where the current is 0.85 p.u. and the electromagnetic torque is 0.78 p.u.

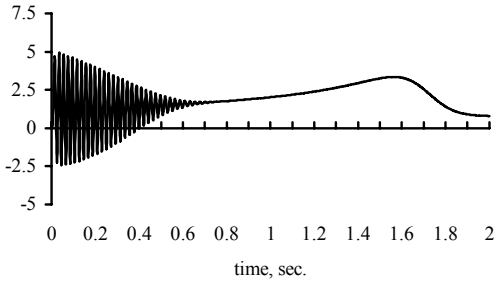

Figure 4: The electromagnetic torque of the wound-rotor motor at start-up with short-circuited starting rheostat

The same tested motor with the same loading conditions is started with speed-controlled starting rheostat. This rheostat is assumed to have four discrete values. The reduction of resistance is accomplished by speed-controlled contactors or common lever.

Figure 5 shows the phase time-domain starting current from which it is obvious that the starting rheostat provides current limiting during starting and acceleration, where the inrush current is 5.54 p.u. and the starting current is about 4.7 p.u. while the starting duration is decreased to 1.34 sec. as shown in figure 6.

Figure 7 shows the electromagnetic torque of the motor at start-up with speed-controlled starting rheostat that provides higher starting torque, where the inrush torque is 7.42 p.u. and the starting torque is about 3.5 p.u. Figure 5, figure 6 and figure 7 show that the steady-state conditions are the same as before.

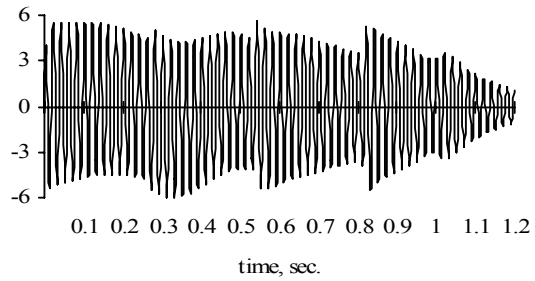

Figure 5: The stator phase current of the wound-rotor motor at start-up with speed-controlled starting rheostat

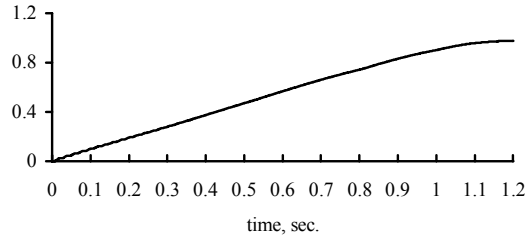

Figure 6: The angular velocity of the wound-rotor motor at start-up with speed-controlled starting rheostat

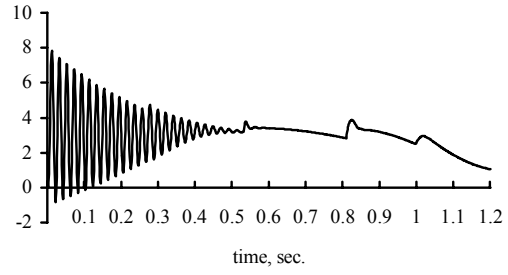

Figure 7: The electromagnetic torque of the wound-rotor motor at start-up with speed-controlled starting rheostat

The spikes seen in the electromagnetic torque of figure 7 are caused by the switching of the starting rheostat as shown in figure 8 and may be undesirable for the driven mechanism. To obtain a smoother starting, the rheostat is to be controlled by the chopper shown in figure 2.

Figure 9 and figure 10 show the phase time-domain starting current and electromagnetic torque at start-up with chopper speed-controlled starting rheostat. The starting process is smoother in comparison with the one observed in figure 5 and figure 7 respectively.

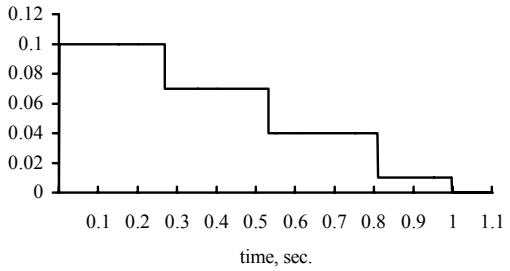

Figure 8: The value of speed-controlled starting rheostat connected to the wound-rotor

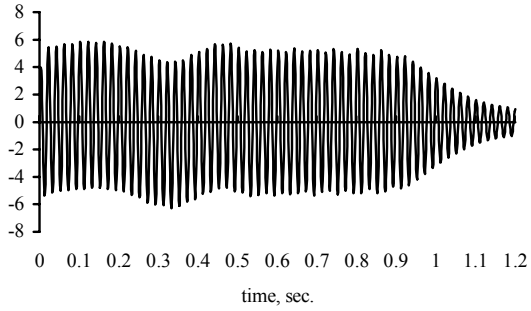

Figure 9: The stator phase current of the wound-rotor motor at start-up with chopper speed-controlled starting rheostat

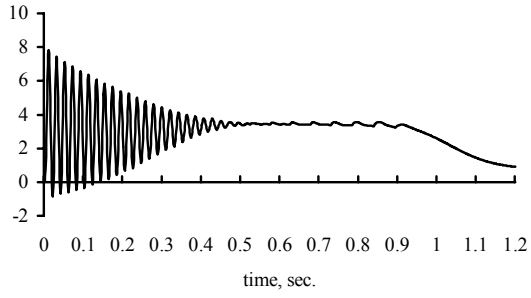

Figure 10: The electromagnetic torque of the wound-rotor motor at start-up with chopper speed-controlled starting rheostat

5. CONCLUSION

A mathematical model for the dynamic simulation of starting and speed control of the wound-rotor induction motor has been developed and experimentally verified. This model consists of a system of differential equations for flux linkages and angular velocity. The number of these differential equations is decreased by one third by using the Cartesian coordinate system. The model allows for the observation of the following variables:

- Stator and rotor currents;
- Active and reactive powers;
- Power factor with which the motor operates;
- Torque and angular velocity;
- Angular rotor position (one more differential equation should be added to the model).

It allows for the dynamic simulation of the following operating conditions:

- Loaded and unloaded starting with current-, speed- or time-controlled starting rheostat;
- Impulse-rheostat speed control;
- Sudden load change (fixed or variable load);
- Short-circuit at the motor terminals;
- Locked rotor.

In addition, the model can be used for the simulation of both transient and steady-state operating conditions, while the use of the Cartesian coordinate system restricts its use only for symmetrical modes of operation.

REFERENCES

Al-Jufout S.A. 1999, "Modelling of Transients and Steady-State Operation of the Induction Motor," In *Proc. 11th European Simulation Symposium*. Society for Computer Simulation International, pp. 670-674, Germany.

Al-Jufout S.A. 2000, "Analysis of the Squirrel-Cage Induction Motor Starting Process on the Basis of Computational Modelling," *Simulation Series,* Society for Computer Simulation International, vol. 32, no. 1, pp. 205-208, USA.

Al-Jufout S.A. 2003, "Dynamic Behavior Analysis of Open-Circuit Transition Wye-Delta Starter," *Pakistan Journal of Applied Sciences,* Asian Network for Scientific Information, vol. 3, no. 8-9, pp. 579-586, Pakistan.

Al-Jufout S.A. 2002, "Modelling of the Autotransformer-Type Reduced-Voltage Starter," In *Proc. 4th International Conference on Quality, Reliability and Maintenance,* Professional Engineering Publishing Limited, University of Oxford, pp. 337-340, UK.

Al-Jufout S.A. 2000, "Computational Modelling for Solid-State Variable-Frequency Induction Motor Drive," In *Proc. 14th European Simulation Multiconference,* Society for Computer Simulation International, pp. 196-200, Belgium.

Al-Jufout S.A. 2000, "Analysis of the Induction Motor Reclosing Process," In *Proc. 2nd Middle East Symposium on Simulation and Modelling,* Society for Computer Simulation International, pp. 115-119, Jordan.

Al-Jufout S.A. 2003, "Modelling of the Cage Induction Motor for Symmetrical and Asymmetrical Modes of Operation," *Computers & Electrical Engineering International Journal*, Pergamon-Elsevier Science Ltd., vol. 29, no. 8, pp. 851-860, UK.

Arkan M., Kostic-Perovic D. and Unsworth P.J. 2005, "Modelling and Simulation of Induction Motors with Inter-Turn Faults for Diagnostics," *Electric Power Systems Research,* vol. 75, no. 1, pp. 57-66.

Ayasun S. and Nwankpa O. 2005, "Induction Motor Tests using MATLAB/Simulink and their Integration into Undergraduate Electric Machinery Courses," *IEEE Transaction on Education,* vol. 48, no. 1, pp. 37-46.

Boglietti A. and Carpaneto E. 2001, "An Accurate Induction Motor High Frequency Model for Electromagnetic Compatibility Analysis," *Electric Power Components and Systems,* vol. 29, pp. 191-209.

Cunha C.C., Lyra R.O. and Filho B.C. 2005, "Simulation and Analysis of Induction Machines with Rotor Asymmetries," *IEEE Transactions on Industry Applications,* vol. 41, no. 1, pp. 18-24.

Elder S., Watson J.F. and Thomson W.T. 1989, "Fault Detection in Induction Motors as a Result of Transient Analysis," In *Proc. 4th International Conference on Electrical Machines and Drives,* pp. 182-186.

Fitzgerald A.E., Kingsley C.Jr. and Umans S. D. 1992, *Electric Machinery*, McGraw Hill, UK.

Hoang L. 2001, "Modelling and Simulation of Electrical Drives Using MATLAB/Simulink and Power System Blockset," In *Proc. 27th Annual Conference of the IEEE Industrial Electronics Society,* vol. 3, pp. 1603-1611.

Khandakji K.A. and Zdrozis K. 2005, "Determination of Quality Parameters of Hoisting Electric Drive Systems with 3-Phase Induction Motors," In *Proc. 5th International Conference on Technology and Automation*, pp. 294-296.

Lagonotte P.T., Miah H.A. and Poloujadoff M. 1999, "Modelling and Identification of Parameters of Saturated Induction Machine Operating under Motor and Generator Conditions," *Electric Power Components and Systems,* vol. 27, pp. 107-121.

O'Sullivan T.M., Schofield N. and Bingham C.M. 2004, "Simulation and Experimental Validation of Induction Machine Dynamics Driving Multi-Inertial Loads," *International Journal of Applied Electromagnetics and Mechanics*, vol. 19, pp. 231-236.

Richard L. and Douglas J. 2002, *Numerical Analysis,* Brooks/Cole Publishing Company, 7th ed. USA.

Seker S. and Ayaz E. 2003, "A Reliability Model for Induction Motor Ball Bearing Degradation," *Electric Power Components and Systems,* vol. 31, pp. 639-652.

Sen, P.C. 1990, "Electric Motor Drives and Control-Past, Present, and Future," *IEEE Transactions on Industrial Electronics.* vol. 37, no. 6, pp. 562-575.

Shi K.L., Chan T.F., Wong Y.K. and Ho S.L. 1999, "Modelling and Simulation of the Three-Phase Induction Motor using Simulink," *International Journal of Electrical Engineering Education,* vol. 36, pp. 163-172.

Wildi T. 2006, *Electrical Machines, Drives and Power Systems.* Prentice Hall, USA.

Zhang C., Meng S., Liu J. and Zhao Z. 2004, "Dynamic Simulation for Induction Motor Vector-Control System," *Journal of University of Science and Technology,* vol. 26, no. 4, pp. 433-437. Beijing.

AUTHORS' BIOGRAPHIES:

Dr. Saleh Abdel-Hamid Al-Jufout received his Ph.D. in Electrical Power Engineering from Donetsk National Technical University. In 1997 he joined Al-Balqa' Applied University then Tafila Technical University in 2005. Currently, he is an associate professor and Dean of Academic Research and Graduate Studies. His research interest includes mathematical modelling of electrical power systems, machines and their protection.

Dr. Kamal Abd Al-Majeed Khandakji received his Ph.D. in Electric Drives and Automation in 1999 from Lvov National Polytechnic University. In 2000, he joined Al-Balqa' Applied University then Tafila Technical University in 2005. Currently, he is an assistant professor at Faculty of Engineering. His research interest includes enhancing the performance of electric drives using microprocessor control, investigation of abnormal modes of power semiconductor drives and visual positioning.